Supporting Information

Quan et al. 10.1073/pnas.1108294109

SI Materials and Methods

Materials. Trypsin (porcine, modified) was from Promega. Acetonitrile (AcN) was from Burdick and Jackson. Titanium dioxide (TiO_2) beads were from a disassembled titanosphere guard column (4 mm inside-diameter x 100 mm, 5 μm, from Inertsil, GL Sciences. GELoader tips were from Eppendorf. The 3 M Empore™ C8 disks were from 3 M Bioanalytical Technologies. All chemicals are analytical grade or better (Merck-Millipore, Sigma, and BDH chemicals).

Antibodies. Anti-syndapin I (mouse monoclonal) was from BD Transduction Laboratories. Anti-syndapin I (goat polyclonal) was from Santa Cruz Biotechnology. Anti-GFP (mouse monoclonal, JL-8 and full-length A.V. rabbit polyclonal) was from Clonetech. Anti-MAP2 (mouse monoclonal) was from Sigma. Texas-red conjugated antimouse secondary antibody was from Jackson Immunoresearch Laboratories.

DNA Plasmids and Recombinant Protein Purification. GST-syndapin I FL-WT (mouse sequence) in pGEX-3X and myc-syndapin I FL-WT (mouse sequence) in pcDNA 3.1-myc were kindly provided by Markus Plomann (University of Cologne, Germany). The full-length sequence was subcloned into pGEX-6P3 (GE Biosciences) and into either pEGFP-C1 (Clonetech) or mCerulean-N1 (1) at the EcoRI restriction enzyme cutting site. The truncated GST- and GFP-tagged syndapin I F-BAR domain (1–304) were generated by subcloning from the full-length construct. The syndapin I point mutants were generated using the Quikchange site-directed mutagenesis kit (Stratagene). The GFP-FBP17 F-BAR (amino acids 1-284) plasmid construct was kindly provided by Pietro De Camilli (Yale University, New Haven, CT). The sequences of all plasmid constructs were confirmed by DNA sequencing. All GST-fusion proteins were expressed in *Escherichia coli* and purified using glutathione (GSH)-sepharose beads (GE Biosciences) and the GST- tag was cleaved from proteins on GSH beads by PreScission protease (GE Biosciences) according to the manufacturer's instructions.

$^{32}P_i$-Labeling of Synaptosomes and Immunoprecipitation of Syndapin I. Crude (P2) synaptosomes were prepared from rat brain and labeled with 0.75 mCi/mL ^{32}Pi (Perkin Elmer Life Sciences) for 1 h at 37 °C as described previously (2). Synaptosomes were lysed in ice cold Lysis Buffer (5 mM Tris pH 7.4, 150 mM NaCl, 1 mM EGTA, 1 mM EDTA, 1% Triton X-100, 1 mM PMSF, 10 μg/mL leupeptin,, Complete EDTA-free protease inhibitor tablets (Roche Applied Science), phosphatase inhibitor cocktail set II (Merck) and centrifuged at 20,442 × *g* for 10 min at 4 °C. Syndapin I was immunoprecipitated from the synaptosomal lysates using 2 μg of anti-syndapin I (BD Transduction Laboratories) monoclonal antibody-conjugated to Protein-G agarose beads (Roche). Beads were washed and eluted in SDS sample buffer and resolved on 20-cm-long 7.5–15% gradient SDS gels. The gel was stained with colloidal Coomassie G-250, dried, and exposed to a PhosphorImager screen to detect incorporated ^{32}P and scanned using the Typhoon Trio (GE Biosciences).

Tryptic Digestion and Phosphopeptide Enrichment. Syndapin I phosphopeptide enrichment and analysis were performed as previously described (3). Syndapin I gel bands, each containing approximately 2 μg of immunopurified protein, were excised from colloidal Coomassie Blue-stained SDS gels. The bands were destained in two washes of 50 mM ammonium bicarbonate in a 50% (v/v) acetonitrile solution 16 h at 4 °C. Destained bands were then dehydrated with 100% acetonitrile solution for 10 min. Syndapin I bands from four different gel lanes were combined as one sample and digested for 16 h at 37 °C in 50 mM ammonium bicarbonate containing 12.5 ng/μL trypsin. The digested solution was then removed and the tryptic peptides remaining in the gel piece were extracted using 60% (v/v) acetonitrile aqueous solution with 15 min vortexing. The combined extract was dried down to 5 μL. Phospho-peptides from the tryptic digest were enriched using TiO_2 as described previously (4) with minor changes. Briefly, the concentrated tryptic digest was added to 25 μL of loading solution [5% (v/v) trifluoroacetic acid in 50% acetonitrile aqueous solution] and loaded onto a GELoader microcolumn tip (Eppendorf) packed with TiO_2 that was washed three times with loading solution. Phospho-peptides were eluted with 20% ammonium hydroxide / 20% acetonitrile aqueous solution and immediately dried. The dried sample was then resuspended in 0.1% formic acid for nano-liquid chromatography tandem mass spectrometry (nano-LC-MS/MS).

Nano-Liquid Chromatography Tandem Mass Spectrometry (LC-MS/MS) and Database Searching. The TiO_2-enriched syndapin I phosphopeptides were analyzed using LC-MS/MS. Briefly, the syndapin I phosphopeptide samples were loaded onto the nano-HPLC system (LC Packings Ultimate HPLC system, Dionex, Netherlands) with a 75-μm inside-diameter precolumn of C18 reversed phase material (ReproSil-Pur 120 C18-AQ, 3-μm beads, Dr Maisch) in 0.1% (v/v) formic acid in water. The samples were eluted through a 50-μm inside-diameter C18 column of the same material at 100 nL/ min. The gradient was from 100% phase A (0.1% formic acid in water) during loading, then increased to 10% phase B (90% acetonitrile, 0.1% formic acid, and 9.9% water) in 3 min, then to 50% phase B in 28 min, then to 60% phase B in 3 min, and finally to 100% phase B in 1 min. The eluate was then sprayed through a 10-μm inside-diameter distal coated SilicaTip (New Objective) into a QSTAR XL quadrupole-TOF MS (AB SCIEX, NW). Information dependent data acquisition was done using a 1 s survey scan from which the three most abundant doubly, triply, or quadruply charged peptides were selected for product ion scans (2 s). For the detection of syndapin I phospho-peptides of a known molecular mass the precursor ion was fixed at the specific m/z setting (2–3 units) using consecutive 2 s scans. The raw data files from the QSTAR XL Q-TOF mass spectrometer were processed into peak lists in Mascot format using the Analyst QS program version 1.1 (AB SCIEX) and the mascot.dll script version 1.6b23 (AB SCIEX and Matrix Science). Database searching was performed using a local copy of Mascot version 2.3.0 (Matrix Science). The searched databases were SwissProt 55.3 (366226 sequences; 132054191 residues) with the taxonomy limited to rodents (6,993 sequences) or SwissProt 56.6 with the taxonomy limited to mammals (64,031 sequences). The database searches were performed with the following variable modifications: deamidation (NQ), oxidation (Met) and phosphorylation (STY) with 250-ppm precursor ion mass tolerance and 0.1-Da mass tolerance for fragment ions. Enzyme specificity for tryptic digests was selected to semitrypsin with two missed cleavages. The Mascot score and expect ratio thresholds were set at greater than 25 and less than 0.05 respectively for a significant peptide to protein match. Peptides were sequenced from the TiO_2-enriched phosphopeptide samples. After sequencing, each identification was aided by Mascot searches, however, each spectrum was also validated manually and ensured that they had sufficient y and b ions for identification and for unambiguous assignment of the phosphorylation site. The Mascot search engine

uses both the +80-Da mass shift and the 98-Da neutral loss for the assignment of a phosphorylation site. We searched for both the +80-Da mass shift and the 98-Da neutral loss in our manual validation of phosphorylation sites using the BioLynx version 1.1 add-on software (AB SCIEX) within the Analyst QS program. Data presented are representative of at least two independent experiments.

Liposome Preparation. Brain L-α-phosphatidyl-L-serine (PS) from Sigma comes as 10 mg/mL chloroform: methanol 95:5 solution. Brain L-α-phosphatidylethanolamine (PE) and brain L-α-phosphatidyl-L-choline (PC) (Sigma) were dissolved in 90:10 (v/v) chloroform: methanol solution. The phospholipids were mixed together as 60% PS, 20% PE, and 20% PC at 100 mg/mL concentration. This percentage composition of liposome mixture was chosen after performing a titration experiment on the acidic phospholipid PS concentration for optimal protein-lipid-binding and was consistent with previous studies (5, 6). The phospholipid mixture was evaporated almost dry under nitrogen flow, leaving about 5–10 μL, resuspended in 1 mL of 20 mM Tris/HCl pH 7.4, 100 mM NaCl and sonicated for 1–2 min on ice for a working solution of 10 mg/mL. The stock solution was freeze/thawed three times with vigorous vortexing on each thaw. Liposomes prepared to this stage were used as the large multilamellar vesicles (LMV). For defined size liposomes (400 and 100 nm), the LMV mixture was filtered through 400 or 100 nm polycarbonate filters (Whatman Cyclopore filters) using an extrusion device (Avanti Polar Lipids) according to the manufacturer's instructions.

Liposome Binding Assay. Purified syndapin I F-BAR proteins (5 μg) were incubated with LMV, 400 or 100 nm liposomes (100 μg) in 50 μL of assembly buffer [20 mM Tris/HCl pH 7.4, 100 mM NaCl, 1 mM EDTA, 1 mM DTT, 1 mM PMSF, and a Complete EDTA-free protease inhibitor cocktail tablet per 50 mL (Roche)] for 15 min at room temperature (RT, 22 °C). The samples were centrifuged at 14,000 × *g* for 15 min to separate lipid-bound (P) and free (S) syndapin I and the fractions analyzed by gel electrophoresis on a 12% SDS-polyacrylamide gel followed by staining with Coomassie blue. Protein gels were scanned on the Typhoon Trio and the protein band intensities were quantified using ImageQuant TL version 2005 (GE Biosciences). The data was expressed as a percentage of protein in the P fraction and normalized to WT protein and statistical analysis was performed using GraphPad Prism 5 (GraphPad Software Inc.).

In Vitro Fluorescence Liposome Tubulation Assay. Purified syndapin I F-BAR proteins (5 μg) were incubated with fluorescent LMV or 400 nm liposomes [100 μg, 60% PS, 20% PC, 10% PE (Sigma), and 10% fluorescein-conjugated PE (Invitrogen)] in 50 μL of assembly buffer for 15 min at RT. The samples were then spotted onto glass slides and examined via fluorescence microscopy. Images presented are representative of three independent experiments.

Protein Sequence, Structure Alignment, and Modeling. Amino acid sequences of the rat, mouse, and human syndapin I F-BAR [PDB ID code 3HAI, (6)] domain and homologous F-BAR domains from human Cdc42 interacting protein 4 [CIP4, PDB ID code 2EFK (7)], human formin-binding protein 17 [FBP17, PDB ID code 2EFL (7)], and human FCH domain only protein 2 [FCHO2, PDB ID code 2V0O (8)] were aligned using T-COFFEE (9). Crystal structures of the syndapin I F-BAR domain and the homologous F-BAR domains as described above were aligned using MUSTANG (10). Modeling of the S76A/E mutations and S76 phosphorylation were completed in vacuo with Sybyl-X 1.2 (www.tripos.com), using the MMFF94 forcefield and default parameters. Figures were prepared with PyMOL (www.pymol.org).

Syndapin I Knockdown in Hippocampal Neurons, Transfections, and Morphological Analysis. Hippocampal neurons were prepared for primary culture using brains from Wistar rat strain at embryo day 18 (E18). For morphological analysis of the hippocampal neurons during development in culture, neurons were cotransfected with GFP-syndapin I FL constructs (1 μg) and syndapin I shRNA (pSUPER neomCerulean vector system, Oligoengine) as previously described (11) to knockdown endogenous syndapin I, by calcium phosphate precipitation at day 4 in vitro (DIV4). Neurons were fixed at DIV6 with 4% paraformaldehyde (PFA) in PBS, pH 7.4 for 8 min at RT 48 h after transfection, immunostained with anti-MAP2 (primary antibody) (Sigma) for 2 h and Texas-red anti-mouse (secondary antibody) (Jackson Immunoresearch Laboratories) for 1 h, and then analyzed via fluorescence microscopy. Images are representative of at least three independent experiments. Morphometric measurements of transiently transfected GFP neurons were performed with the neurite outgrowth module in Metamorph acquisition and analysis software version 7.7 (Molecular Devices) from at least three independent experiments. The quantitation for the number of total neurite outgrowths from the neuron cell body, the average neurite length, and total branching points were determined from total of 30–45 neurons for each condition in the knockdown-rescue experiments and 45–80 neurons for each condition in the GFP overexpression experiments. Statistical analysis was performed using GraphPad Prism 5.

Fluorescence Microscopy and Imaging. Fluorescence microscopy and imaging for the various assays were performed as follows unless otherwise specified. Images were collected using Metamorph acquisition software version 7.7 (Molecular Devices), an Olympus IX81 Motorized Inverted Microscope, a Hamamatsu ORCA-ERG (Hamamatsu Photonics), 12 bit FireWire Cooled CCD Camera and either a UPLAPO100XOI3, UPLAPO60XOI3, or UPLAPO40XOI3 objective. All images were cropped to size and each fluorochrome was adjusted using identical settings for brightness and contrast to represent the observed images. Where applicable, Z stacks were collected at 0.5 μm intervals (approximately five images/stack) and 3D deconvoluted using AutoDeblur version 9.3.1 (AutoQuant Imaging, Inc.). A maximum projection image was then generated.

Circular Dichroism (CD) Analysis of Syndapin I F-BAR Mutant Proteins. CD spectra for mouse syndapin I F-BAR domain residues 1–304 were collected for the WT, T181A, T181E, S76A, and S76E mutant proteins. Proteins were in 10 mM potassium phosphate pH 7.4, 50 mM Na_2SO_4 at 0.495 mg/mL, 0.385 mg/mL, 0.165 mg/mL, 0.165 mg/mL and 0.193 mg/mL, respectively. Samples were centrifuged for 1 min in a bench top micro centrifuge before a 300-μL aliquot was transferred to the microcuvette and equilibrated in the CD sample chamber for 5 min. CD spectra were collected on a J-815 CD spectrophotometer (Jasco) with a scanning range 260 nm to 180 nm, 20 nm/ min, data pitch, 0.5 nm at a temperature of 21 ° C. The CD output for each of the F-BAR domain mutants were converted to text and analyzed with Microsoft Excel. Data was simplified to only include the range 190 nm to 240 nm with 1-nm steps as was required by the K2D2 software (12). The data for each mutant was normalized by expressing the delta epsilon values as a percentage of the maximum delta epsilon value for each dataset. A scaling factor of 24 was then applied to bring the spectra into an appropriate scale for analysis. Individual spectra were analyzed with the K2D2 software to calculate the relative percentage of alpha helix and beta sheet for each mutant.

Coimmunoprecipitation of GFP-Tagged Syndapin I F-BAR Phospho-mutants and myc-Tagged Syndapin I FL and Western Blot Analysis. COS7 cells were cultured in 100 mm dishes to 80% confluency then cotransfected with the GFP-tagged syndapin I F-BAR (GFP-Sdpn I

F-BAR) mutant constructs (5 μg) and myc-tagged syndapin I FL-WT (5 μg) using FuGENE 6 (Roche) according to the manufacturer's protocol. All conditions were carried out in duplicate for each independent experiment. After 24 h transfection, cells were placed on ice and washed 4 times with ice cold PBS. Total cell lysates were prepared by incubating cells for 10 min with Lysis Buffer (20 mM Tris pH 7.4, 150 mM NaCl, 1 mM EGTA, 1 mM EDTA, 1% Triton X-100, 1 mM PMSF, 10 μg/ml leupeptin, Complete protease inhibitor tablets EDTA-free, phosphatase inhibitor cocktail set II). The mixture was then centrifuged at 14,000 × *g* for 10 min and the supernatant was harvested as the total cell lysate. For the coimmunoprecipitation, the total cell lysate from each condition was incubated with 2 μg of anti-GFP (JL-8) mouse monoclonal antibody (Clonetech) preconjugated to Protein-G agarose beads (Roche) for 3 h. The immunoprecipitate on beads were washed four times with ice cold PBS and the sample was eluted with SDS sample buffer. The total cell lysates and eluates were resolved on a 12% SDS-polyacrylamide gel and then transferred onto Protran immobilized nitrocellulose membrane (PerkinElmer). To detect the transfected GFP-syndapin I F-BAR protein, the membranes were probed with anti-GFP mouse monoclonal antibody. The secondary antibody was goat anti-mouse polyclonal antibody-conjugated to HRP (Dako) and the signal was developed with SuperSignal West Pico chemiluminescence (Thermofisher Scientific). The membranes were then stripped with 0.2 M NaOH and reprobed for myc-sdpn I FL protein using anti-syndapin I mouse monoclonal antibody (BD Biosciences) and developed as above. It should be noted that the anti-syndapin I mouse monoclonal antibody does not detect the syndapin I protein truncated at the F-BAR domain (1–304). Western blots were scanned using the BioRad GS800 Densitometer (BioRad).

Syndapin I Knockdown in Cerebellar Granule Neurons and Measuring Dextran Uptake. Primary cultures of cerebellar granule neurons (CGNs) were prepared from the cerebella of seven-day-old Sprague Dawley rat pups as previously described (13). Syndapin expression was silenced using a modified pSUPER vector system (pSUPER neoGFP, Oligoengine) as previously described (11). The CGNs were cotransfected with shRNA (0.8 μg/well) and syndapin I-mCer (1 μg/well) constructs on day 5 or 6 using calcium phosphate precipitation (13). Uptake of tetramethylrhodamine-dextran (40 kDa) (Invitrogen) was monitored as described previously (14). CGNs (72 hours posttransfection) were left for 10 min in incubation medium (in mM: 170 NaCl, 3.5 KCl, 0.4 KH_2PO_4, 20 TES (*N*-tris[hydroxy-methyl]-methyl-2-aminoethanesulfonic acid), 5 $NaHCO_3$, 5 glucose, 1.2 Na_2SO_4, 1.2 $MgCl_2$, 1.3 $CaCl_2$, pH 7.4) and then mounted in a Warner imaging chamber (RC-21BRFS). The CGNs were then stimulated with a train of 800 action potentials (80 Hz 10 s). Tetramethylrhodamine-dextran (50 μM) was present during the stimulus and was washed away immediately after stimulation. The chamber was mounted on a Zeiss (Germany) Axiovert (Observer D1) epifluorescence microscope and CGNs were viewed with a 40X oil immersion objective at 550 nm excitation and >575 nm emission. Dextran uptake was visualized using a Hamamatsu Orca-ER CCD digital camera and offline imaging software (Simple PCI, Compix Imaging Systems). The extent of dextran loading was determined by the number of fluorescent puncta per neuron.

Generation of Phospho-T181 Specific Polyclonal Antibody. The polyclonal antibody that recognizes T181 phosphorylated (pT181) syndapin I was generated by injecting rabbits with four doses at 500 μg every three weeks (IMVS Veterinary Services Division) of the synthetic peptide C-TEQSV*pT*PEQQK conjugated to diptheria toxoid (Auspep Pty Ltd.). The antiserum was affinity purified with Protein-G agarose beads according to manufacturer's protocol (Roche). Western blot analyses were used to test the phospho-specificity of both the antiserum and affinity purified pT181 antibody on syndapin I immunopurified (using anti-syndapin I mouse monoclonal antibody) from brain and synaptosomes, in the presence or absence of 50 units of antarctic phosphatase (New England Biolabs) treatment to dephosphorylate the immunopurified syndapin I (Fig. S8*A*). Total syndapin I protein was detected with an anti-syndapin I goat polyclonal antibody.

In Vitro Phosphorylation of Syndapin I F-BAR with PKC and CKII. Purified syndapin I F-BAR-WT and phospho-deficient mutants (2 μg) were phosphorylated with purified rat brain PKC (30 ng, Calbiochem) or rat liver CKII (Promega) in buffer containing 30 mM Tris-HCl (pH 7.4), 1 mM $MgSO_4$, 1 mM EGTA, and 80 μM [γ-^{32}P]ATP (10 μCi) for 10 min at 37 °C. For PKC phosphorylation, 40 μg/mL of PS cofactor were also added to each reaction mix. Reactions were terminated by cooling and the addition of SDS, and resolved on 20-cm-long 7.5–15% gradient SDS gels. The gel was stained overnight with colloidal Coomassie G-250 stain and scanned using a flatbed scanner. The gel was dried and exposed to a PhosphorImager screen to detect incorporated ^{32}P and scanned using the Typhoon Trio (GE Biosciences).

1. Rizzo MA, Springer GH, Granada B, Piston DW (2004) An improved cyan fluorescent protein variant useful for FRET. *Nat.Biotechnol* 22:445–449.
2. Robinson PJ, et al. (1993) Dynamin GTPase regulated by protein kinase C phosphorylation in nerve terminals. *Nature* 365:163–166.
3. Graham ME, et al. (2007) The in vivo phosphorylation sites of rat brain dynamin I. *J.Biol.Chem* 282:14695–14707.
4. Larsen MR, Thingholm TE, Jensen ON, Roepstorff P, Jorgensen TJ (2005) Highly selective enrichment of phosphorylated peptides from peptide mixtures using titanium dioxide microcolumns. *Mol Cell Proteomics* 4:873–886.
5. Itoh T, et al. (2005) Dynamin and the actin cytoskeleton cooperatively regulate plasma membrane invagination by BAR and F-BAR proteins. *Dev Cell* 9:791–804.
6. Wang Q, et al. (2009) Molecular mechanism of membrane constriction and tubulation mediated by the F-BAR protein Pacsin/Syndapin. *Proc Natl Acad Sci USA* 106:12700–12705.
7. Shimada A, et al. (2007) Curved EFC/F-BAR-domain dimers are joined end to end into a filament for membrane invagination in endocytosis. *Cell* 129:761–772.
8. Henne WM, et al. (2007) Structure and analysis of FCHo2 F-BAR domain: A dimerizing and membrane recruitment module that effects membrane curvature. *Structure* 15:839–852.
9. Notredame C, Higgins DG, Heringa J (2000) T-Coffee: A novel method for fast and accurate multiple sequence alignment. *J Mol Biol* 302:205–217.
10. Konagurthu AS, Whisstock JC, Stuckey PJ, Lesk AM (2006) MUSTANG: A multiple structural alignment algorithm. *Proteins* 64:559–574.
11. Cheung G, Jupp OJ, Cousin MA (2010) Activity-dependent bulk endocytosis and clathrin-dependent endocytosis replenish specific synaptic vesicle pools in central nerve terminals. *J Neurosci* 30:8151–8161.
12. Perez-Iratxeta C, Andrade-Navarro MA (2008) K2D2: Estimation of protein secondary structure from circular dichroism spectra. *BMC Struct Biol* 8:25.
13. Tan TC, et al. (2003) Cdk5 is essential for synaptic vesicle endocytosis. *Nat Cell Biol* 5:701–710.
14. Clayton EL, et al. (2009) The phospho-dependent dynamin-syndapin interaction triggers activity-dependent bulk endocytosis of synaptic vesicles. *J Neurosci* 29:7706–7717.

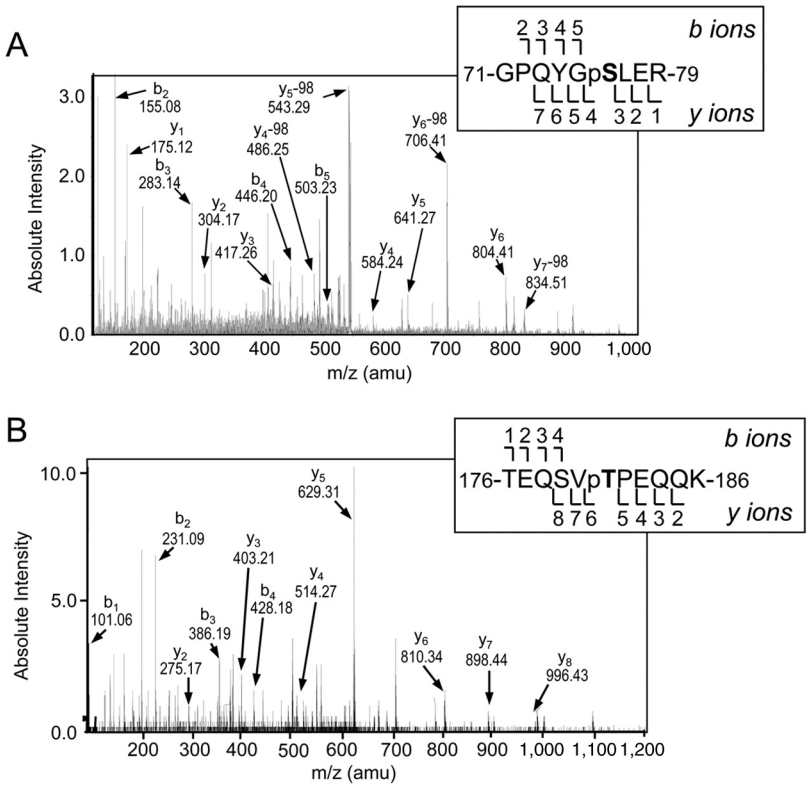

Fig. S1. Phosphorylation site assignment of S76 and T181 by LC-MS/MS in synaptosomes and brain tissue. (*A* and *B*) The two syndapin I phospho-peptides were purified from total tryptic digests using TiO_2 microcolumns and subjected to direct sequencing of the phosphorylation sites using MS/MS. (*A*) The precursor ion at *m/z* 543.77 $[M + 2H]^{2+}$ was selected for LC-MS/MS sequencing and was determined to be monophosphorylated syndapin I 71–79 (1,085.45 Da). Analysis of the y and b product ions allowed the unambiguous assignment of S76 (shown as pS in the sequence above the panel) as the phosphorylation site. (*B*) The precursor ion *m/z* 677.87 $[M + 2H]^{2+}$ was selected for LC-MS/MS sequencing and was determined to be monophosphorylated syndapin I 176–186 (1,353.58 Da). The phosphorylation site was unambiguously determined to be T181 (shown as pT in the sequence above panel). Fragment ions showing both +80-Da mass shift and neutral loss of phosphoric acid (−98 Da) are shown.

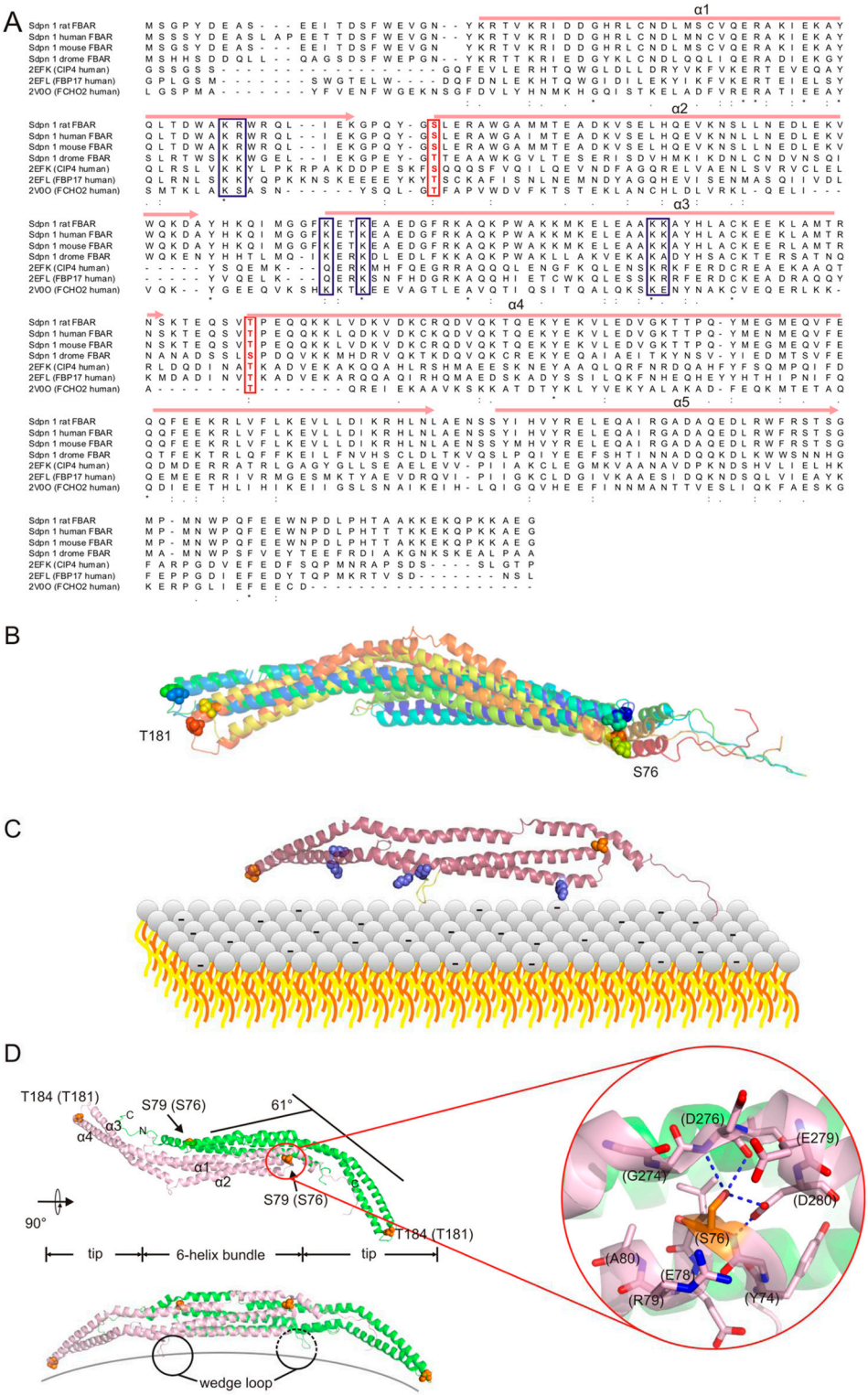

Fig. S2. Location of S76 and T181 phosphosites on the syndapin I F-BAR domain crystal structure. (*A*) Amino acid sequence alignment of the F-BAR domains of rat, human, and mouse syndapin I with homologous F-BAR domains; CIP4, FBP17, FCHO2. This alignment was done by T-COFFEE. S76 and T181 are highlighted in red boxes and residues involved in lipid bilayer interactions are highlighted in blue boxes. (*B*) Ribbon representation of the structure-based alignment of human syndapin I (orange), rat FBP17 (blue), rat CIP4 (green), and human FCHO2 (yellow). The conserved phosphorylation sites are shown in the colored spheres. (*C*) Modeling of the syndapin I F-BAR dimer structure relative to a hydrophobic lipid membrane layer orientating the positions of the basic lipid-binding Arg and Lys residues (blue spheres) and the S76 and T181 phosphosites (orange spheres). (*D*) The human syndapin I F-BAR domain dimer (PDB ID code 3HAI) and the positions of the S76 and T181 phosphosites. Zoomed panel showing the residues and H-bonds surrounding S76. Note that the sequence of rat and human syndapin I differ such that rat S76 is S79 in humans, and rat T181 is T184 in humans. For consistency we retain the numbering of the rat sequence when describing the human syndapin I crystal structure. The "wedge loop" is an eight-residue-long insertion in helix α-2 previously proposed (6) to intercalate into lipid bilayer and function as a wedge for membrane bending.

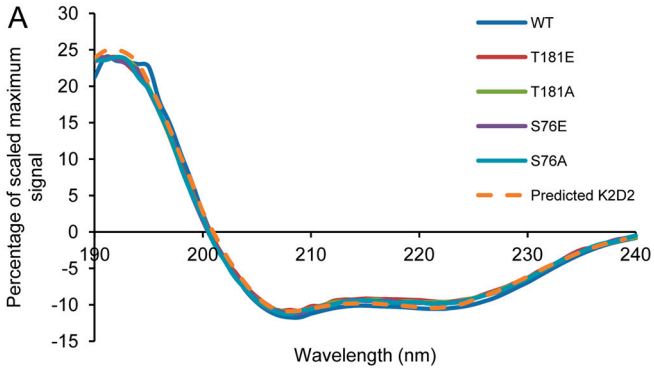

B

Protein	WT	T181E	T181A	S76E	S76A
Est. % helix	81.81	77.73	77.73	77.73	77.73
Est. % Sheet	0.66	0.72	0.72	0.72	0.72

Fig. S3. S76 and T181 phosphosite mutations do not affect the helical folding of recombinant syndapin I F-BAR domain. (*A*) Circular dichroism (*CD*) spectra of syndapin I F-BAR domain WT and mutant proteins expressed as a percentage of maximum delta epsilon value and then multiplied by a scale factor of 24 to best suit input into K2D2 secondary structure prediction software (12). (*B*) Delta epsilon values were entered into K2D2 for each mutant and compared to a reference database to estimate the percentage of alpha helix and beta sheet for each of the mutants. The estimated percentage of alpha helix for each of the four mutants is consistent with that of the WT enzyme. Each of the F-BAR domain protein CD spectra data curve agrees well with the predicted CD curve in K2D2 (orange dashed line).

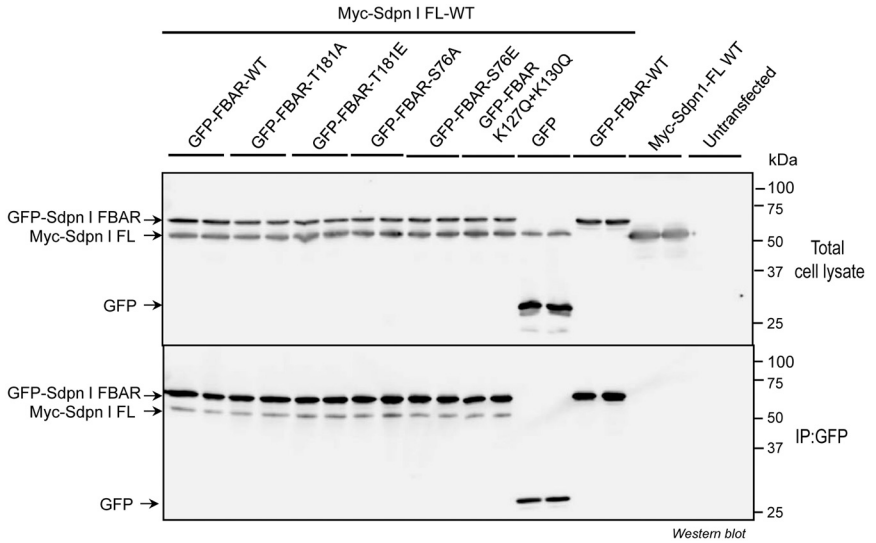

Fig. S4. Syndapin I F-BAR phosphosite mutants do not affect self dimerization. Myc-tagged syndapin I full-length wild-type (Myc-Sdpn I FL-WT) and GFP-tagged syndapin I F-BAR (GFP-Sdpn I F-BAR) phospho-mutants and lipid-binding mutant (K127Q+K130Q) were co-overexpressed in COS7 cells. The total overexpressed myc-tagged syndapin I and GFP-tagged syndapin I F-BAR mutants protein levels were detected with anti-syndapin I (only detects full-length syndapin I) and anti-GFP monoclonal antibodies, respectively (*Top*), to show equivalent levels of protein expression between the mutant constructs. Immunoprecipitation of GFP-syndapin I F-BAR mutants (*Bottom*) followed by Western blotting for GFP and syndapin I shows that the phospho-mutants do not affect syndapin self-oligomerization via the F-BAR domain. Blots are representative of three independent experiments.

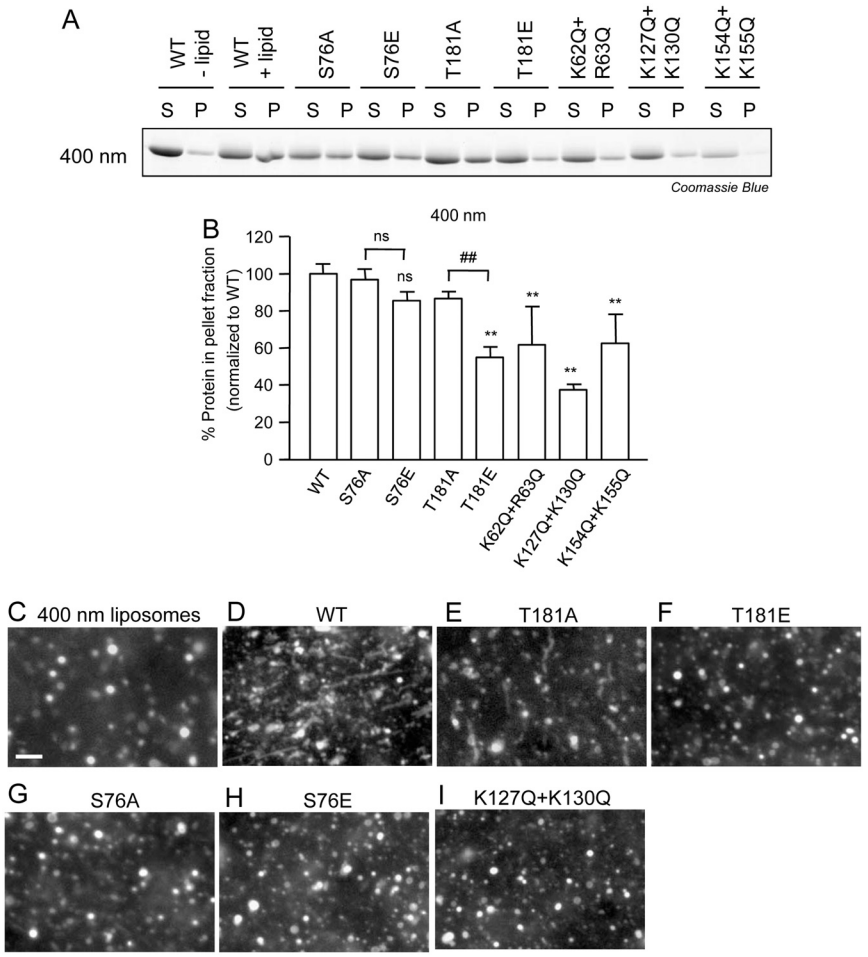

Fig. S5. Effects of syndapin I F-BAR phosphosites mutants on lipid-binding and tubulation are dependent on liposome size. (*A*) Purified protein (5 μg) of the syndapin I F-BAR domain phospho-mutants and lipid-binding mutants were incubated with extruded 400-nm liposomes (50 μg) made of 60% PS, 20% PC, and 20% PE. Samples were centrifuged and the supernatant (S) and pellet (P) fractions analyzed using SDS/PAGE followed by Coomassie Blue staining. (*B*) Quantitative representation of *A*. Three independent experiments were performed and the protein band intensity was measured. The error bars indicate standard error of the mean (±SEM, $n = 3$). A one-way analysis of variance (ANOVA) was applied. (*C–I*) Extruded 400-nm liposomes (50 μg) containing 60% PS, 20% PC, 10% PE and 10% fluorescein-conjugated PE were incubated with purified syndapin I F-BAR domain phospho-mutants and lipid-binding mutants and analyzed using fluorescence microscopy for lipid tubules. Scale bar, 10 μm. Images are representative of three independent experiments.

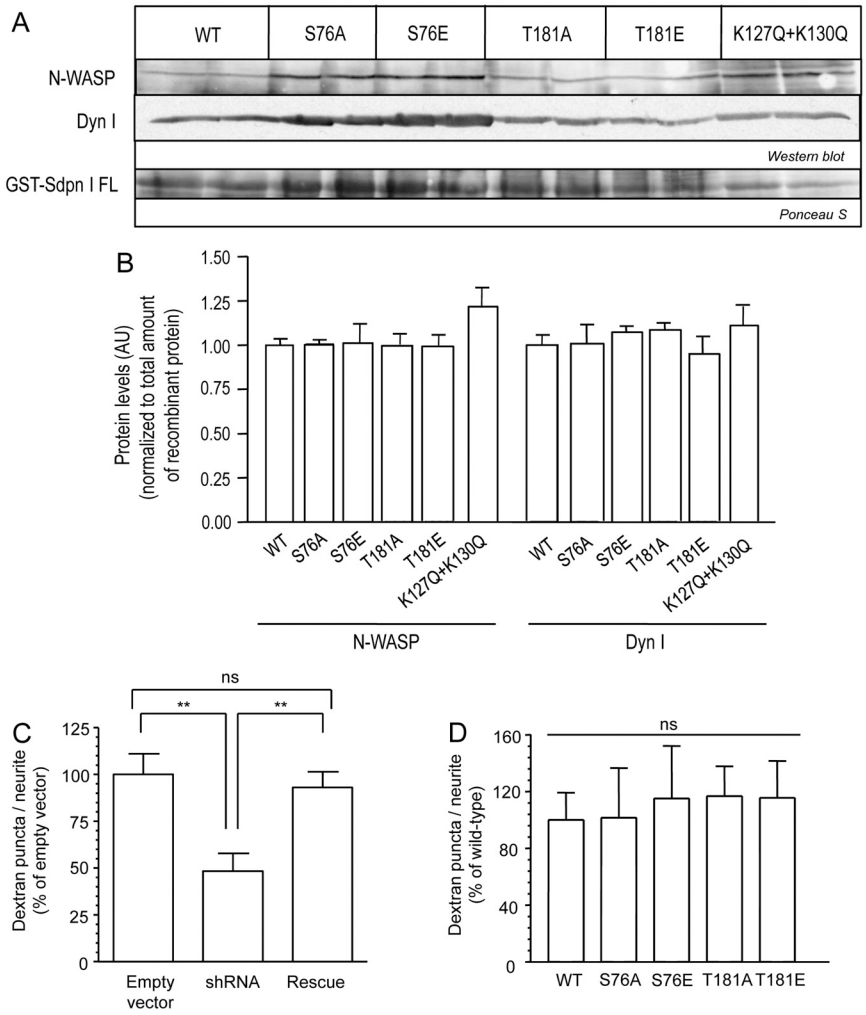

Fig. S6. Syndapin I F-BAR phosphosite mutants do not regulate dynamin I and N-WASP binding, and ADBE. GST-tagged syndapin I full-length (GST-Sdpn I FL) phospho-mutants and lipid-binding mutant (K127Q+K130Q) were used to pulldown binding proteins in whole brain cell extracts. (*A*) The binding partners, dynamin I (dyn I) and N-WASP were detected using Western blotting. The total amount of GST-tagged fusion protein used for the pulldown assay is shown with Ponceau S stain. (*B*) Quantitative analysis of the amount of protein pulled down with each construct. The protein levels (±SD, $n = 2$) are normalized to total amount of GST-tagged fusion protein and expressed as a relative amount to the WT protein. (*C*) Primary cultures of neurons (CGNs) were transfected with either empty shRNA vector, shRNA vector containing syndapin I oligo (shRNA), or syndapin I shRNA vector coexpressed with wild-type (WT) syndapin I-mCer vector (rescue). After 72 h transfection CGNs were stimulated by a train of 800 action potentials (80 Hz) in the presence of 50 μM tetramethylrhodamine-dextran followed by immediate washout. The amount of dextran uptake is expressed as the number of dextran puncta per neuron as a percentage of empty vector. Total $n = 25$, 20 and 21 neurons ±SEM for the empty vector, shRNA and rescue, respectively, from at least six independent experiments; $** P < 0.01$, one-way ANOVA. (*D*) CGNs were cotransfected with the shRNA syndapin vector and either WT- syndapin-mCer or phospho-mutants of the syndapin F-BAR domain (S76A, S76E, T181A, T181E). Dextran uptake was quantified as in *C*. Results are expressed as dextran puncta per neuron as a percentage of the wild-type syndapin rescue. $n \geq 7$ neurons ±SEM; one-way ANOVA.

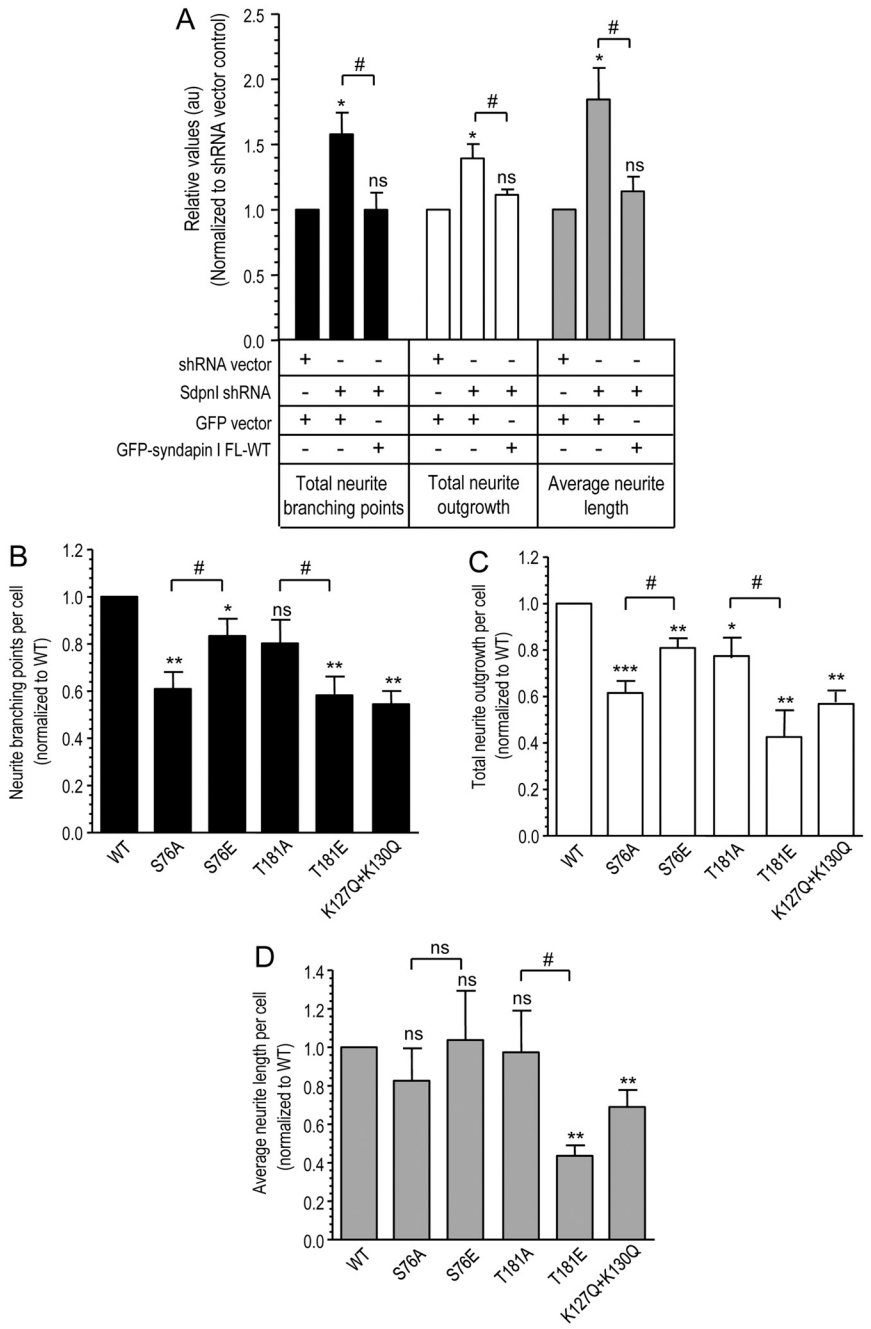

Fig. S7. Syndapin I F-BAR phosphosites do not rescue syndapin I knockdown phenotype in hippocampal neurons. (*A*) Primary rat hippocampal neurons were cotransfected at DIV4 with a shRNA-mCerulean targeting endogenous syndapin I (Sdpn I) and either RNAi-resistant GFP-syndapin I FL-WT or phospho-mutants then processed for immunofluorescence microscopy at DIV6. Quantitative analysis of the morphological effects per neuron cotransfected with either control shRNA vector and GFP vector, or Sdpn I shRNA and GFP vector, or Sdpn I shRNA and GFP-syndapin I FL-WT , for total neurite outgrowth, total neurite branching points, and average length of neurite outgrowth from the cell body. There was no differentiation between axons or dendrites in the morphological analysis of the neurites. Relative mean values (±SEM) are normalized and expressed as a ratio to control shRNA vector cotransfected with GFP vector from at least three independent experiments. (*B–D*) Rescue of the syndapin I knockdown phenotypes with F-BAR phosphosite mutants. Neuronal phenotypes were quantified relative to the WT rescue phenotype shown in panel A (SdpnI shRNA + GFP-syndapin I FL-WT) for neurite branch points per cell (*B*), total neurite outgrowth per cell (*C*), and average neurite length per cell (*D*). Relative mean values (±SEM) are from at least three independent experiments. For all quantitative analysis, a total of 30–45 neurons for each condition were analyzed. A one-way analysis of variance (ANOVA) was applied: $***P < 0.0001$, $**P < 0.001$, $*P < 0.05$, ns = non-significant against syndapin I F-BAR WT. Student's *t* test was applied between shRNA knockdown and GFP-syndapin I FL-WT rescue, and between phospho-deficient A and phospho-mimetic E mutants $\#P < 0.05$.

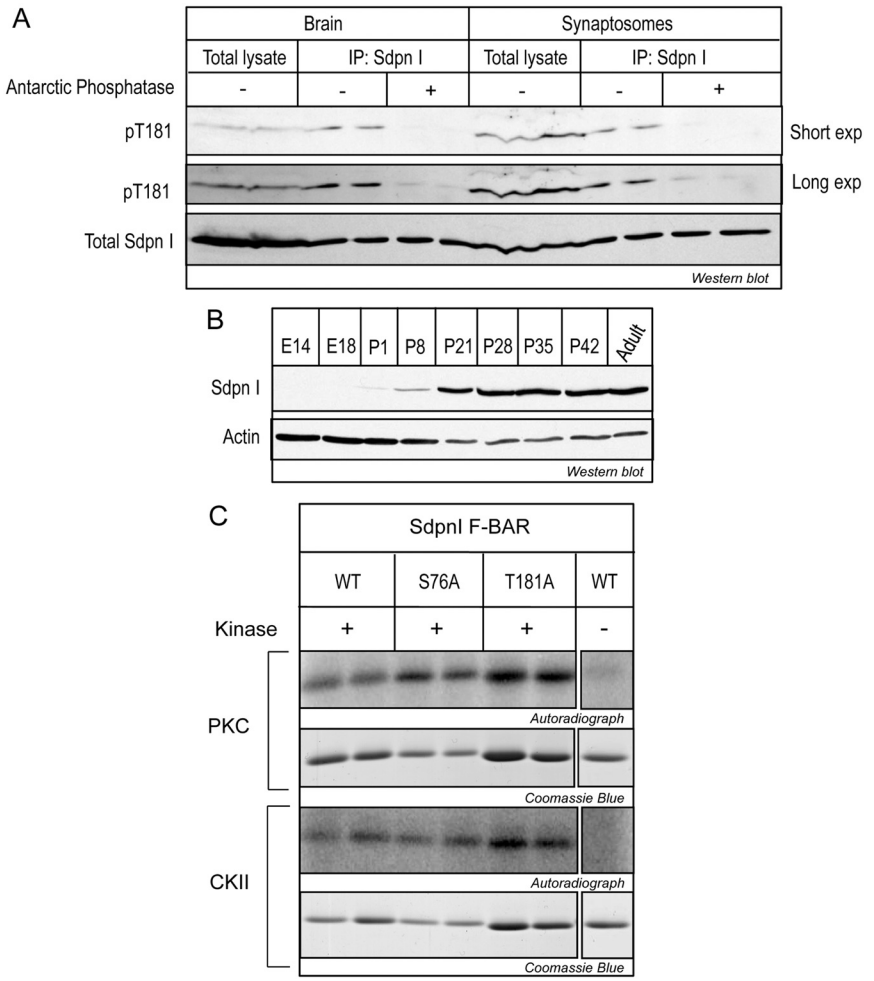

Fig. S8. Syndapin I pT181 phospho-specific polyclonal antibody, syndapin I expression during brain development, and in vitro phosphorylation by PKC or CKII. (*A*) Western blot analyses of total brain and synaptosome lysates (50 μg), and immunoprecipitated (IP) syndapin I (Sdpn I), in the absence or presence of 50U of antarctic phosphatase to determine the phospho-specificity of the generated rabbit polyclonal syndapin I phospho-T181 (pT181) antibody. A short and long film exposure time is shown to demonstrate the pT181 antibody only detected phosphorylated syndapin I. Total syndapin I protein levels were detected using an anti-syndapin I mouse monoclonal antibody (BD Biosciences). Note: the total brain and synaptosome lanes were overloaded to detect the pT181 in the lysates. Hence, in subsequent experiments, to detect pT181 we immunoprecipitated syndapin I to enrich for the phosphosite. (*B*) Western blot analyses of total brain lysates (20 μg) from rats at the indicated developmental ages. Actin was used as protein level control. Blots presented are representative of three independent experiments. (*C*) Purified syndapin I F-BAR-WT and phospho-deficient mutants (S76A and T181A) were phosphorylated with either purified PKC or CKII for 10 min at 37 °C. Samples were resolved by SDS/PAGE, protein was stained by Coomassie Blue and ^{32}P-labeled syndapin I F-BAR was visualized by autoradiography. Control conditions with the absence of either kinase with WT protein show that purified syndapin I F-BAR does not auto-phosphorylate. Reactions were performed in duplicates and images are representative of two independent experiments.

Table S1. Summary of effects of S76 and T181 phosphosites on syndapin I function

	Lipid-binding			Lipid tubulation		Neuronal morphogenesis		
F-BAR construct	LMV	400 nm	100 nm	LMV	400 nm	Total neurite outgrowth	Total neurite branching	Average neurite length
WT	Yes	Yes	Yes	Long	Short	↑↑	↑↑↑	-
S76A	Yes	Yes	Yes	Short	No	-	-	-
S76E	Yes	Yes	↓	Short	No	-	-	-
T181A	Yes	Yes	Yes	Long	Short	-	-	-
T181E	↓	↓↓	↓↓	No	No	↓↓↓	↓↓↓	↓↓
K127Q+K130Q	↓↓	↓↓↓	↓↓↓	No	No	↓↓↓	↓↓↓	↓↓
K62Q+K63Q	↓↓	↓↓	↓↓	No	No	-	-	-
K154Q+K155Q	↓↓	↓↓	↓↓	No	No	-	-	-

Summary of the effects of S76 (light gray) and T181 (dark gray) phosphosite mutants and double Lys lipid-binding mutants in the in vitro lipid-binding and tubulation assays using LMV, 400-nm, and 100-nm liposomes (composed of 60% PS, 20% PC, and 20% PE) and effects on neurite development in cultured hippocampal neurons. The number of "↓" and "↑" symbols indicates the relative levels of reduction and increase (quantitated in Fig. 3 *B* and *C*, Fig. 6 *H–J*, and Fig. S5*B*) of the mutants compared with WT protein.